Heat Shock Factor 1 Dynamically Restructures the Yeast Genome

Surabhi Chowdhary[1], Amoldeep S. Kainth[1] and David S. Gross*

Department of Biochemistry and Molecular Biology
Louisiana State University Health Sciences Center
Shreveport, LA 71130

[1]Equal Contribution.

*Correspondence: dgross@lsuhsc.edu

SUMMARY

Transcriptional induction of *Heat Shock Protein* (*HSP*) genes is accompanied by dynamic changes in their 3D structure and spatial organization, yet the molecular basis for these striking phenomena remains unknown. Using chromosome conformation capture and single cell imaging, we show that Heat Shock Factor 1 (Hsf1)-activated genes in *Saccharomyces cerevisiae* rapidly and reversibly coalesce into intranuclear foci, while genes activated by Msn2 and Msn4, alternative thermal stress-responsive activators, do not. Likewise, constitutively expressed genes do not coalesce, even those interposed between *HSP* genes. Stress-activated Hsf1 coalesces into discrete subnuclear puncta, and in concert with its target *HSP* genes, de-coalesces and disperses into the nucleoplasm upon transcriptional attenuation. Hsf1 is both necessary and sufficient for driving gene coalescence, whereas RNA Pol II is necessary but not sufficient. Our findings reveal that gene coalescence is activator-dependent and refute models which posit that gene repositioning is a general feature of transcriptional activation.

Keywords

Hsf1; Msn2/Msn4; Gene interaction; chromosomal clustering; transcription factories; nuclear foci; phase separation; 3D genome; budding yeast

INTRODUCTION

Increasing evidence suggests that nuclear processes such as transcription, recombination, replication and repair can be influenced not only by local chromatin structure but also by three-dimensional genome architecture. Genomes of higher eukaryotes are compartmentalized into discrete structural and regulatory units termed topologically associating domains (TADs) (reviewed inDekker and Mirny, 2016; Hnisz et al., 2016a; Wendt and Grosveld, 2014). Genes located within these structures tend to have similar expression states and epigenetic signatures, and perturbation of TAD integrity may lead to aberrant activation (Flavahan et al., 2016; Hnisz et al., 2016b; Lupianez et al., 2015). Recent studies using genome-wide 3C-based techniques have unveiled spatial genomic structures analogous to mammalian TADs in budding yeast (Eser et al., 2017; Hsieh et al., 2015).

Within TADs, transcriptional enhancers are brought into physical contact with the promoters of nearby or distant genes via looping of the intervening DNA. Enhancer-promoter loops, typically 10-100 kb in mammals, are stabilized by Mediator, cohesin, and the sequence-specific factor YY1 (Beagan et al., 2017; Kagey et al., 2010; Weintraub et al., 2017). Analogous, albeit smaller, enhancer (UAS)-promoter loops have been observed in *S. cerevisiae* (Chowdhary et al., 2017; Dobi and Winston, 2007). Physical contacts between the 5' and 3' ends of actively transcribed genes, as well as between gene regulatory elements and actively transcribed coding sequences, have also been observed in yeast (Chowdhary et al., 2017; Hampsey et al., 2011) as well as in mammals (Beagrie et al., 2017; Lee et al., 2015).

Importantly, DNA loops tend to be dynamic, and such dynamism facilitates long-range chromosomal interactions. For example, chromosome conformation capture (3C)-based techniques have shown that both proximal and distal actively transcribed mammalian genes engage in frequent contacts that may contribute to their co-regulation (Fanucchi et al., 2013; Li et al., 2012; Rao et al., 2014; Zhang et al., 2013). Moreover, activated mammalian genes have been observed to reposition themselves into discrete sites of

intense RNA synthesis termed “transcription factories” (Osborne et al., 2004; Papantonis et al., 2012; Papantonis et al., 2010; Park et al., 2014; Schoenfelder et al., 2010). In these and other examples, it is thought that increased transcription is fostered by high local concentrations of RNA Pol II and pre-mRNA processing factors present in stable substructures (Feuerborn and Cook, 2015). However, a single molecule analysis using super-resolution microscopy indicated that Pol II clusters form transiently, with their mean lifetime increasing upon transcriptionally stimulating conditions (Cisse et al., 2013). It therefore remains unclear whether all transcriptionally active genes cluster, whether such clustering is the cause or consequence of transcription, and whether this mode of transcriptional control exists in eukaryotes other than mammals.

A powerful model with which to study dynamic DNA looping and genome restructuring is the heat shock (HS)-responsive family of genes in *S. cerevisiae*. Many of these genes, including those encoding molecular chaperones and cytoprotective heat shock proteins (HSPs), are under the regulation of Heat Shock Factor 1 (Hsf1), an evolutionarily conserved, gene-specific activator (Morimoto, 1998). Genes under the regulation of Hsf1 undergo dramatic transformations in chromatin structure upon their activation. These alterations include gene-wide disassembly of nucleosomes (Zhao et al., 2005) and substantial increases in Hsf1, Mediator, SAGA and Pol II occupancy (Fan et al., 2006; Kim and Gross, 2013; Kremer and Gross, 2009). Additionally, striking increases in intragenic and intergenic chromosomal contacts of *HSP* genes accompany their activation. These alterations include DNA looping between UAS and promoter, promoter and terminator (gene looping), and flanking regulatory regions and coding sequences (gene ‘crumpling’). Activated *HSP* genes also engage in frequent *cis*- and *trans*-interactions with each other, coalescing into transcriptionally active foci (Chowdhary et al., 2017). It is unclear what underlies these profound genomic rearrangements. It is also unclear whether gene clustering is the default state for transcriptional control in budding yeast, as suggested for mammalian cells.

In the work reported here, we demonstrate that stress-activated Hsf1 is a key determinant driving yeast genes into a coalesced state. Heat-shock-responsive genes

regulated by alternative activators – Msn2 and Msn4 – do not detectably cluster, nor do coordinately regulated ribosomal protein genes. While high levels of transcription are necessary for coalescence, they are not sufficient. Our results argue against the idea that gene repositioning is a general feature of transcriptional activation and instead point to activators such as Hsf1 as the drivers of global genome restructuring.

RESULTS

HSP Gene Coalescence Is Strikingly Specific and Robust

HSP genes engage in extensive intra- and interchromosomal interactions upon their heat shock-induced activation (Chowdhary et al., 2017) (see, e.g., Figures 2B and S2A below). If *HSP* gene coalescence is biologically significant, then one might predict that non-*HSP* genes would be excluded from such clustering, even those residing in close linear proximity. To test this, we used a highly sensitive form of 3C, termed Taq I - 3C (Chowdhary et al., 2017), to investigate intergenic interactions within a 35 kb domain on Chr. XII. Three *HSP* genes – *UBI4*, *HSP104* and *SSA2* – lie within this domain and each is occupied by Hsf1, whose abundance substantially increases in cells exposed to acute heat shock (30° to 39°C shift for 5 min) as revealed by ChIP-seq (Figure 1A). Under non-heat shock (NHS) conditions, no 3C interactions could be detected between these genes (Figure 1B (blue matrix); gene regions defined in Figures S1A and S1B), consistent with their low basal transcription (Figure S4B and D. Pincus et al, in preparation [Reviewer's Appendix, Panel A]) and previous nucleosome-resolution chromatin contact analysis indicating that these genes lie within separate chromosome interaction domains (CIDs) (Hsieh et al., 2015).

However, following heat shock, not only did neighboring *HSP104* and *SSA2* engage in intense interactions, but *UBI4* frequently contacted both genes (Figure 1B (red matrices)). This is despite the fact that *UBI4* is separated from the former by 25 kb, a distance encompassing six CIDs (Hsieh et al., 2015), and from the latter by 33 kb, encompassing eight CIDs (Figure S2B). By contrast, the constitutively active and crumpled gene *FRA1*, located between *UBI4* and *HSP104*, engaged in no detectable

interactions with *HSP104, UBI4* or *SSA2* under either condition (Figure 1B). Likewise, *PAU17*, a non-*HSP* gene interposed between *HSP104* and *SSA2*, failed to engage in physical interactions with either gene. Thus, both *PAU17* and *FRA1*, despite being transcriptionally active and residing in close proximity to the *HSP* genes, are excluded from the heat shock-mediated coalescence taking place between them.

Given the remarkable specificity of *HSP* intergenic interaction, we wished to know how robust such interactions might be. To do so, we asked whether Hsf1-regulated genes residing on the left arm of Chr. XII would physically interact with *TMA10*, a gene located on the distal right arm and inducibly occupied by Hsf1 (Figures 1C, 1D). Genome-wide 3C-based analyses have indicated that the left and right ends of Chr. XII are physically isolated from each other, due to a "near absolute" barrier conferred by the 100-200 rDNA repeats that assemble into the nucleolus (Duan et al., 2010; Rutledge et al., 2015). Consistent with these prior studies, Taq I - 3C failed to detect above-background interaction between *HSP104 - TMA10* or *SSA2 - TMA10* in non-induced cells (Figure 1E, *left*). However, following a 10 min heat shock, physical interactions between these Hsf1 targets were readily detectable (Figure 1E, *right*). While it is possible that these intrachromosomal interactions are facilitated by loss of nucleolar integrity, fluorescence microscopy of acutely heat-shocked cells expressing an RFP-tagged nucleolar protein argues otherwise (Figure S2C). Our results thus indicate that *HSP* gene interactions are not only remarkably specific, but sufficiently robust to circumvent the physical barrier imposed by the nucleolus.

Heat Shock-Induced Coalescence Is Distinct to Genes Regulated by Hsf1

Is gene coalescence a general feature of heat-shock-activated genes or is it a distinctive attribute of Hsf1-regulated genes? To address this, we examined genes whose thermal-responsive regulation is under the control of Msn2 (and its paralogue, Msn4). Msn2/4 regulates the transcription of 200-300 genes in response to a variety of environmental stresses, including heat, oxidative, osmotic and salt stress (Elfving et al., 2014; Gasch et al., 2000). We selected three genes – *CTT1*, *PGM2* and *RTN2* – whose thermal stress-dependent transcription is independent of Hsf1 (Figure S3A [Reviewer's

Appendix, Panel B]) (Solis et al., 2016). Chromosome conformational analysis revealed the presence of heat-shock-dependent intragenic looping and crumpling interactions within all three Msn2/4 target genes (Figure S3B; gene maps in Figure S1C), consistent with the notion that such restructuring is characteristic of actively transcribed genes (Chowdhary et al., 2017). Nonetheless, using primers corresponding to the UAS, 5'-end, mid-ORF and 3'-end of each gene, we were unable to detect above-background interactions between *CTT1*, *PGM2* and *RTN2* upon their transcriptional activation (Figure 2A) despite the presence of readily detectable interactions between Hsf1 target genes (Figures 2B, S2A) in the same cells. We additionally tested the interaction between heat shock-induced Hsf1 and Msn2/Msn4-target genes, yet no above-background interaction could be detected (Figure 2C).

We next asked if constitutively active genes coalesce, and tested intergenic interactions between two coordinately regulated ribosomal protein genes, *RPL10* and *RPL22A*, as well as between two unrelated genes, *FAS2* and *RPL10*. Each gene is heavily transcribed under NHS conditions, as assayed by nascent and steady-state RNA measurements (D. Pincus et al, in preparation [Reviewer's Appendix, Panel C]). Nonetheless, no above-background interactions could be detected (Figure S3C). Thus, by the criterion of Taq I - 3C, heat shock-inducible, Msn2/4-regulated genes fail to coalesce with each other, as do other highly expressed, coordinately regulated genes. These observations raise the possibility that Hsf1-regulated genes may be distinctive.

To further demonstrate this distinctiveness, we performed single-cell fluorescence microscopy analysis of *lacO*-tagged genes in heterozygous diploids. This revealed that *HSP104-lacO*$_{256}$ and *HSP12-lacO*$_{128}$, residing on Chr. XII and Chr. VI, respectively, coalesced under acute heat shock conditions (2.5 or 10 min heat shock), and the frequency of such coalescence was significantly higher than in either the control or 30 min heat-shock state (Figure 2D (*solid bars)*; examples shown in Figure S3D). This is in agreement with the notion that *HSP* gene coalescence is highly dynamic, detectable within 60 sec of heat shock, yet evanescent (Chowdhary et al., 2017). In contrast, only background levels of coalescence (possibly reflecting coincidental overlap) were observed between Hsf1-regulated *HSP104* and Msn2-regulated *PGM2* (Figure 2D,

striped bars). Moreover, while under non-inducing conditions the distance between *HSP104* and *HSP12* was normally distributed, following acute heat shock the distribution was skewed towards shorter distances (Figure 2E), consistent with interchromosomal clustering of the two loci. No such change was observed between *HSP104* and *PGM2* in identically treated cells. Collectively, 3C and microscopy analyses suggest that (i) unlike Hsf1-regulated genes, those under the control of Msn2/4 do not coalesce – either with themselves or with Hsf1-targets – in response to heat shock; and (ii) Hsf1 targets do not generally coalesce with other transcriptionally active genes, even those induced by thermal stress. These observations argue that coalescence is a distinguishing feature of Hsf1-activated genes.

Hsf1, But Not Msn2, Forms Discrete Intranuclear Puncta in Cells Exposed to Thermal Stress

To address the possibility that Hsf1 itself coalesces upon activation, we imaged live cells harboring Hsf1-GFP. As shown in Figure 2F, Hsf1 is largely nuclear and diffusely localized under NHS conditions. Following brief exposure (6 - 16 min) to thermal stress (38°C), Hsf1 forms discrete intranuclear puncta (submicrometer bodies). Following a longer exposure (36 - 66 min), the Hsf1 puncta dissolve, and the distribution of intranuclear Hsf1 once again returns to a diffuse state, closely paralleling the kinetics of *HSP* gene coalescence and de-coalescence (Figures 2D and 2E) (Chowdhary et al., 2017). If the formation of Hsf1 puncta reflects coalescence of its gene targets, then it might be predicted that Msn2, despite strongly activating transcription in response to heat shock (Figure S3A [Reviewer's Appendix, Panel B]), will not itself coalesce. As shown in Figure 2F, Msn2-GFP, largely cytoplasmic in NHS cells (0 min), translocates to the nucleus under acutely stressful conditions (4.5 min), consistent with previous reports (Chi et al., 2001; Gorner et al., 1998). In contrast to Hsf1, the intranuclear distribution of Msn2 remains diffuse throughout the heat shock time course (Figure 2F, 4.5 - 45 min). Notably, exposure to 8.5% ethanol has similar effects, including the transient formation of Hsf1 puncta (L.S. Rubio, A.S.K. and D.S.G., unpubl. observations), so the ability/inability to form puncta appears to be an inherent property of Hsf1 and Msn2 activation.

Hsf1 Is Both Necessary and Sufficient to Drive Coalescence of a Pol II Gene

To more directly test the importance of Hsf1 in driving changes in *HSP* gene conformation and 3D nuclear organization, we conditionally depleted it from the nucleus using the Anchor Away technique (Haruki et al., 2008). Growth of *HSF1-FRB* cells on rapamycin demonstrates that Hsf1 is essential for viability, even at 30°C (Figure 3A), consistent with previous observations (Sorger and Pelham, 1988). Cytoplasmic sequestration of Hsf1-FRB, achieved by pre-exposure of cells to rapamycin for 90 min, drastically reduced Hsf1-FRB occupancy of representative *HSP* genes following a subsequent 10 min heat shock (Figure 3B, light blue bars). Consistent with Hsf1's central role in regulating these genes (Solis et al., 2016), Pol II occupancy and transcript accumulation were likewise severely reduced (Figures S4A and S4B [Reviewer's Appendix, Panel A]).). Concomitant with this reduction in transcription, formation of 5'-3' gene loops was obviated, as were other intragenic interactions including UAS - promoter looping (Figure 3C, pink bars). In conjunction, intergenic coalescence was reduced to background levels (Figure 3D). As expected, neither looping nor crumpling of constitutively expressed *BUD3* was affected by this perturbation (Figure S4D). Therefore, Hsf1 is required to drive its target genes into a looped, crumpled and coalesced state in response to heat shock.

To test whether DNA-bound Hsf1 is sufficient to cause an otherwise unrelated gene to coalesce with *HSP* genes, we chromosomally integrated a high-affinity Hsf1 binding site (the UAS_{HS} of *HSP82*) upstream of *BUD3*, creating an allele termed UAS_{HS}-*BUD3* (Figures 3E and S5A). We then conducted 3C analysis on both non-induced and acutely heat-shock-induced cells. As shown in Figure 3F, Hsf1 strongly occupied UAS_{HS}-*BUD3* but not *BUD3* in response to a 10 min heat shock. Moreover, UAS_{HS}-*BUD3* exhibited increased levels of intragenic interactions (looping and crumpling) following heat shock (Figure 3G), consistent with increased transcription and Pol II abundance within the coding region (A.S.K. and D.S.G., unpubl. observations). In addition and even more striking, UAS_{HS}-*BUD3* engaged in *de novo* intergenic interactions with both *HSP104* and *HSP82* (Figures 3H, *right* and S5B), again in marked contrast to the wild-type gene (Figure 3H, *left*). Therefore, Hsf1 can reprogram the

genomic organization and 3D nuclear location of a heterologous gene in response to heat shock.

To address the corollary question, does removal of Hsf1 lead to loss of coalescence without a concomitant loss of transcription, we analyzed an Hsf1-, Msn2/4-coregulated gene, *HSP12*, in an Hsf1 Anchor Away strain. *HSP12* has an extended gap-type HSE (consisting of TTCn-NNNNN-nTTCn-NNNNN-nTTC) lying ~800 bp upstream of its TSS that is inducibly occupied by Hsf1 (Figure 4A, *right*). It also has seven stress-response elements (STREs) – CCCCY motifs – recognized by Msn2/Msn4 located between the HSE and TSS (schematically illustrated in Figure 4A). Conditional nuclear depletion of Hsf1 caused a modest reduction in heat shock-induced transcription of *HSP12*, based on both RT-qPCR and RNA-seq analyses (Figure S4C [Reviewer's Appendix, Panel A]). Likewise, this perturbation caused a parallel reduction in heat shock-induced gene looping and crumpling (Figure 4B), yet it obviated *HSP12* interactions with *HSP104*, *HSP82* and *SSA2* altogether (Figure 4C). Thus, although *HSP12* transcription remains high upon Hsf1 depletion, its interchromosomal interactions with other *HSP* genes are abolished. This observation demonstrates that a high level of *HSP* gene transcription, while strongly correlated with intragenic looping, can be uncoupled from *HSP* gene coalescence.

Pol II Is Necessary But Not Sufficient For *HSP* Gene Coalescence

Finally, we asked whether Pol II, in particular its largest subunit (Rpb1), is required for the striking changes observed in *HSP* gene conformation and nuclear organization. If such changes were dependent on Pol II, then anchoring away Rpb1 should obviate looping, crumpling and coalescence. Rapamycin-induced cytoplasmic sequestration of Rpb1 rendered cells inviable on solid medium (Figure S6A). In cells pre-exposed to rapamycin for 60 min, Rpb1 occupancy of heat shock-induced *HSP* gene promoters and coding regions was greatly reduced (Figure 4D, light blue bars), although notably this nuclear depletion had little or no effect on Hsf1 occupancy (Figure S6B). Nonetheless, all intragenic interactions tested were greatly diminished by prior removal of Rpb1, including UAS-promotor looping (Figure 4E, first pairwise test of each gene), implicating

Pol II in the stable formation of such loops. Concomitant with loss of intragenic looping was loss of all tested intergenic interactions (Figure 4F, pink bars), implicating Pol II in the coalescence of *HSP* genes. As expected, both looping and crumpling interactions at *BUD3* were strongly diminished by Rpb1 depletion (Figure S6C). Therefore, Pol II is critical for the formation of novel *cis*- and *trans*-intergenic interactions characteristic of activated *HSP* genes, yet even high levels of it – as inferred from intragenic looping and expression assays (Figures 4B, 4C, S3A, S3B, S6C and D. Pincus, in preparation [Reviewer's Appendix]) – are not sufficient.

DISCUSSION

Hsf1 Target Genes Distinctively Coalesce Upon Their Activation

We present evidence that physical interactions between heat shock-activated Hsf1 target genes, located on the same or different chromosomes, are remarkably specific and robust. Genes interposed between Hsf1 targets are excluded from these interactions, yet *HSP* genes separated by the "near absolute" barrier of the nucleolus (Duan et al., 2010; Rutledge et al., 2015) readily interact. Moreover, not all heavily transcribed genes coalesce, even those whose transcription is activated by alternative thermal stress-responsive activators. Likewise, coordinately regulated ribosomal protein genes show no detectable interaction despite the fact that those tested lie on the same chromosome and are separated by only 20 kb. The latter observation is consistent with recent genome-wide 3C analyses that failed to uncover significant interactions between Pol II genes across the yeast genome under control (NHS) conditions (Duan et al., 2010; Rutledge et al., 2015).

What distinguishes a coalescing from a non-coalescing gene, therefore, is not whether it is coordinately regulated, transcribed at a high level, or induced by heat shock. What dictates coalescence is whether a gene is regulated by Hsf1. Indeed, using a combination of conditional Hsf1 nuclear depletion and ectopic Hsf1 targeting, we have demonstrated that Hsf1 is both necessary and sufficient to drive a transcriptionally competent Pol II gene into a coalesced state. We are unaware of any other yeast

activator that possesses comparable activity. The closest example may be that of an erythroid-specific transcription factor, Klf1. Using a combination of 3C, ChIP-3C, FISH and immunofluorescence, Fraser and colleagues have shown that in mouse erythroid cells, Klf1-regulated globin genes relocate into transcription factories where they engage in preferential (although not exclusive) interchromosomal associations with other Klf1-regulated genes (Schoenfelder et al., 2010). Thus, Klf1 drives *preferential* physical interactions between its target genes in response to a developmental signal; evidence reported here suggests that Hsf1 drives *exclusive* interactions between its target genes in response to an environmental signal. Hi-C and/or ChIA-PET analysis will be required to show this definitively, however.

Is *HSP* Gene Coalescence Related to Other Examples of Gene Clustering or to Repositioning of Active Genes to the Nuclear Periphery?

As alluded above, a particularly striking aspect of our study is that constitutively active genes (*PAU17* and *FRA1*), despite located in close linear proximity to *HSP* genes, do not coalesce with them. Such specificity contrasts with a recent report of methionine-responsive genes in yeast that engage in intrachromosomal clustering upon their induction as assessed by 3C, yet unlike what we observed here, unrelated neighboring genes also tended to interact (Du et al., 2017). More similar to the specificity and selectivity of Hsf1-target gene coalescence are observations that TNFα-responsive genes in human endothelial cells engage in intrachromosomal interactions upon cytokine stimulation (Papantonis et al., 2010), whereas an actively transcribed gene interposed between them, and located nearby to one of them, is excluded from such colocalization (Fanucchi et al., 2013).

In addition, microscopy and biochemical analysis have shown that *GAL* genes relocate to the nuclear pore complex (NPC) upon galactose induction (Casolari et al., 2004). Such repositioning has been reported to be accompanied by sustained clustering of *GAL* alleles, initially at the NPC and subsequently in the nucleoplasm, as detected by a microscopy-based analysis (resolution of ~500 nm) (Brickner et al., 2016). However, no

evidence of *GAL1-10* allelic interaction was seen in galactose-induced diploids using either Hi-C (Kim et al., 2017) or wide-field fluorescence localization microscopy (Backlund et al., 2014). Therefore, it is unclear whether repositioning of the *GAL* locus to the NPC is related to the robust and intricate physical interactions that we detect between *HSP* genes using 3C, whose resolution is ~1-5 nm (Dekker and Mirny, 2016). In a similar vein, earlier studies on the effect of heat shock on human nuclear substructure reported the existence of "stress bodies." As these stress bodies appear to be arrays of HSF1 bound to repetitive DNA sequences that are spatially independent from *HSP* gene transcription (Jolly et al., 1997; Metz et al., 2004), they are unlikely to be related to the concerted coalescence of *HSP* genes reported here.

Evanescent coalescence between Hsf1 target genes contrasts with prevailing models suggesting that actively transcribed genes relocate into statically assembled substructures (Feuerborn and Cook, 2015). Our observations more strongly resemble the dynamic assembly of Pol II clusters in serum-stimulated human cells (Cisse et al., 2013) or the dynamic sorting of immunoglobulin genes residing on different chromosomes into transcription factories during mouse B-cell development (Park et al., 2014).

Is *HSP* Gene Coalescence an Example of Phase Separation?

Recently, phase separation of multi-molecular assemblies has been suggested as a mechanism for transcriptional control (Hnisz et al., 2017). We have described observations consistent with the *HSP* regulon undergoing a liquid-liquid phase separation in response to heat shock. In particular, we have observed that genes sharing in common only the identity of the DNA-bound transcription factor nucleate into foci under activating conditions. While such coalescence accompanies heightened expression of these genes – and Pol II transcription is indeed required for *HSP* coalescence (this study; (Chowdhary et al., 2017)) – intensity of transcription cannot be the only parameter dictating foci formation. Nascent RNA measurements in acutely heat-shocked cells reveal that Msn2/Msn4-regulated *CTT1* and *PGM2* are expressed at levels that equal or exceed several Hsf1 targets studied here, including *HSP12*, *UBI4*

and *TMA10* (D. Pincus et, in preparation [Reviewer's Appendix]). Yet *CTT1* and *PGM2* do not detectably interact with one another, nor with representative *HSP* genes.

Why then do Hsf1-regulated genes coalesce, while Msn2/Msn4-regulated genes do not? One possibility is that Hsf1 recruits a distinct set and/or quantity of coactivators, in particular Mediator, which is prominently recruited to *HSP* genes (Anandhakumar et al., 2016; Fan et al., 2006; Kim and Gross, 2013). Notably, Mediator is nearly undetectable at comparably activated *CTT1* and *RPL* genes (Fan et al., 2006); such relative scarcity may reflect its transient association with those loci (Jeronimo and Robert, 2014; Wong et al., 2014). Stable association of Mediator at Hsf1 regulated genes may be a key to *HSP* gene coalescence and putative phase separation given the abundance of intrinsically disordered regions (IDRs) within this coactivator (Toth-Petroczy et al., 2008) (see also Reviewer's Appendix Panel D). IDRs in the abundant nuclear protein HP1 appear to contribute to phase separation of constitutive heterochromatin domains in human and *Drosophila* (Larson et al., 2017; Strom et al., 2017). Therefore, Hsf1-Mediator complexes, along with other covalently modified chromatin-associated proteins and/or nascent RNA transcripts that comprise multivalent networks (Hnisz et al., 2017), may act in a concerted fashion to drive *HSP* gene coalescence in yeast. Our future efforts will explore these and other intriguing possibilities.

EXPERIMENTAL PROCEDURES

Yeast Strains

Strain construction details are provided in Supplemental Experimental Procedures. Yeast strains used in this study are listed in Table S1; primers used for strain construction are provided in Table S6.

Chromosome Conformation Capture (3C)

Taq I - 3C was conducted as previously described (Chowdhary et al., 2017). Primers used are listed in Tables S2 and S3.

Chromatin Immunoprecipitation (ChIP)

ChIP was performed essentially as previously described (Chowdhary et al., 2017). Primers used are listed in Table S4.

Reverse Transcription-qPCR (RT-qPCR)

RT-qPCR was performed as previously described (Chowdhary et al., 2017). Primers used are listed in Table S5.

Further methods can be found in Supplemental Experimental Procedures.

SUPPLEMENTAL INFORMATION

Supplemental Information includes six figures and six tables.

AUTHOR CONTRIBUTIONS

S.C., A.S.K. and D.S.G. designed the project. S.C and A.S.K. conducted the investigation. S.C., A.S.K. and D.S.G analyzed the data. S.C. and A.S.K. made the figures. D.S.G., S.C and A.S.K. wrote the paper.

ACKNOWLEDGEMENTS

We thank Jayamani Anandhakumar and Michael Guertin for experimental and bioinformatics assistance, respectively; David Pincus for stimulating discussions and for sharing unpublished results; Kelly Tatchell for assistance with fluorescence microscopy; Ishita Ghosh for construction of IGY101; and Jason and Donna Brickner, Frank Holstege and Francois Robert for generously providing yeast strains.

REFERENCES

Anandhakumar, J., Moustafa, Y.W., Chowdhary, S., Kainth, A.S., and Gross, D.S. (2016). Evidence for multiple Mediator complexes in yeast independently recruited by activated Heat Shock Factor. Mol Cell Biol *36*, 1943–1960.

Backlund, M.P., Joyner, R., Weis, K., and Moerner, W.E. (2014). Correlations of three-dimensional motion of chromosomal loci in yeast revealed by the double-helix point spread function microscope. Mol Biol Cell *25*, 3619-3629.

Beagan, J.A., Duong, M.T., Titus, K.R., Zhou, L., Cao, Z., Ma, J., Lachanski, C.V., Gillis, D.R., and Phillips-Cremins, J.E. (2017). YY1 and CTCF orchestrate a 3D chromatin looping switch during early neural lineage commitment. Genome research *27*, 1139-1152.

Beagrie, R.A., Scialdone, A., Schueler, M., Kraemer, D.C., Chotalia, M., Xie, S.Q., Barbieri, M., de Santiago, I., Lavitas, L.M., Branco, M.R.*, et al.* (2017). Complex multi-enhancer contacts captured by genome architecture mapping. Nature *543*, 519-524.

Brickner, D.G., Sood, V., Tutucci, E., Coukos, R., Viets, K., Singer, R.H., and Brickner, J.H. (2016). Subnuclear positioning and interchromosomal clustering of the GAL1-10 locus are controlled by separable, interdependent mechanisms. Mol Biol Cell *27*, 2980-2993.

Casolari, J.M., Brown, C.R., Komili, S., West, J., Hieronymus, H., and Silver, P.A. (2004). Genome-wide localization of the nuclear transport machinery couples transcriptional status and nuclear organization. Cell *117*, 427-439.

Chi, Y., Huddleston, M.J., Zhang, X., Young, R.A., Annan, R.S., Carr, S.A., and Deshaies, R.J. (2001). Negative regulation of Gcn4 and Msn2 transcription factors by Srb10 cyclin-dependent kinase. Genes Dev *15*, 1078-1092.

Chowdhary, S., Kainth, A.S., and Gross, D.S. (2017). Heat shock protein genes undergo dynamic alteration in their three-dimensional structure and genome organization in response to thermal stress. Mol Cell Biol *37*, e00292-00217.

Cisse, II, Izeddin, I., Causse, S.Z., Boudarene, L., Senecal, A., Muresan, L., Dugast-Darzacq, C., Hajj, B., Dahan, M., and Darzacq, X. (2013). Real-time dynamics of RNA polymerase II clustering in live human cells. Science *341*, 664-667.

Dekker, J., and Mirny, L. (2016). The 3D Genome as Moderator of Chromosomal Communication. Cell *164*, 1110-1121.

Dobi, K.C., and Winston, F. (2007). Analysis of transcriptional activation at a distance in Saccharomyces cerevisiae. Mol Cell Biol *27*, 5575-5586.

Du, M., Zhang, Q., and Bai, L. (2017). Three distinct mechanisms of long-distance modulation of gene expression in yeast. PLoS Genet *13*, e1006736.
Duan, Z., Andronescu, M., Schutz, K., McIlwain, S., Kim, Y.J., Lee, C., Shendure, J., Fields, S., Blau, C.A., and Noble, W.S. (2010). A three-dimensional model of the yeast genome. Nature *465*, 363-367.
Elfving, N., Chereji, R.V., Bharatula, V., Bjorklund, S., Morozov, A.V., and Broach, J.R. (2014). A dynamic interplay of nucleosome and Msn2 binding regulates kinetics of gene activation and repression following stress. Nucleic Acids Res *42*, 5468-5482.
Erkine, A.M., Magrogan, S.F., Sekinger, E.A., and Gross, D.S. (1999). Cooperative binding of heat shock factor to the yeast *HSP82* promoter *in vivo* and *in vitro*. Mol Cell Biol *19*, 1627-1639.
Eser, U., Chandler-Brown, D., Ay, F., Straight, A.F., Duan, Z., Noble, W.S., and Skotheim, J.M. (2017). Form and function of topologically associating genomic domains in budding yeast. Proc Natl Acad Sci U S A *114*, E3061-E3070.
Fan, X., Chou, D.M., and Struhl, K. (2006). Activator-specific recruitment of Mediator in vivo. Nature structural & molecular biology *13*, 117-120.
Fanucchi, S., Shibayama, Y., Burd, S., Weinberg, M.S., and Mhlanga, M.M. (2013). Chromosomal contact permits transcription between coregulated genes. Cell *155*, 606-620.
Feuerborn, A., and Cook, P.R. (2015). Why the activity of a gene depends on its neighbors. Trends Genet *31*, 483-490.
Flavahan, W.A., Drier, Y., Liau, B.B., Gillespie, S.M., Venteicher, A.S., Stemmer-Rachamimov, A.O., Suva, M.L., and Bernstein, B.E. (2016). Insulator dysfunction and oncogene activation in IDH mutant gliomas. Nature *529*, 110-114.
Gasch, A.P., Spellman, P.T., Kao, C.M., Carmel-Harel, O., Eisen, M.B., Storz, G., Botstein, D., and Brown, P.O. (2000). Genomic expression programs in the response of yeast cells to environmental changes. Mol Biol Cell *11*, 4241-4257.
Gorner, W., Durchschlag, E., Martinez-Pastor, M.T., Estruch, F., Ammerer, G., Hamilton, B., Ruis, H., and Schuller, C. (1998). Nuclear localization of the C2H2 zinc finger protein Msn2p is regulated by stress and protein kinase A activity. Genes Dev *12*, 586-597.
Hampsey, M., Singh, B.N., Ansari, A., Laine, J.P., and Krishnamurthy, S. (2011). Control of eukaryotic gene expression: gene loops and transcriptional memory. Adv Enzyme Regul *51*, 118-125.
Haruki, H., Nishikawa, J., and Laemmli, U.K. (2008). The anchor-away technique: rapid, conditional establishment of yeast mutant phenotypes. Mol Cell *31*, 925-932.
Hnisz, D., Day, D.S., and Young, R.A. (2016a). Insulated Neighborhoods: Structural and Functional Units of Mammalian Gene Control. Cell *167*, 1188-1200.
Hnisz, D., Shrinivas, K., Young, R.A., Chakraborty, A.K., and Sharp, P.A. (2017). A Phase Separation Model for Transcriptional Control. Cell *169*, 13-23.
Hnisz, D., Weintraub, A.S., Day, D.S., Valton, A.L., Bak, R.O., Li, C.H., Goldmann, J., Lajoie, B.R., Fan, Z.P., Sigova, A.A.*, et al.* (2016b). Activation of proto-oncogenes by disruption of chromosome neighborhoods. Science *351*, 1454-1458.
Hsieh, T.H., Weiner, A., Lajoie, B., Dekker, J., Friedman, N., and Rando, O.J. (2015). Mapping nucleosome resolution chromosome folding in yeast by Micro-C. Cell *162*, 108-119.

Jeronimo, C., and Robert, F. (2014). Kin28 regulates the transient association of Mediator with core promoters. Nat Struct Mol Biol *21*, 449-455.
Jolly, C., Morimoto, R., Robert-Nicoud, M., and Vourc'h, C. (1997). HSF1 transcription factor concentrates in nuclear foci during heat shock: relationship with transcription sites. Journal of cell science *110*, 2935-2941.
Kagey, M.H., Newman, J.J., Bilodeau, S., Zhan, Y., Orlando, D.A., van Berkum, N.L., Ebmeier, C.C., Goossens, J., Rahl, P.B., Levine, S.S.*, et al.* (2010). Mediator and cohesin connect gene expression and chromatin architecture. Nature *467*, 430-435.
Kim, S., and Gross, D.S. (2013). Mediator recruitment to heat shock genes requires dual Hsf1 activation domains and Mediator Tail subunits Med15 and Med16. J Biol Chem *288*, 12197-12213.
Kim, S., Liachko, I., Brickner, D.G., Cook, K., Noble, W.S., Brickner, J.H., Shendure, J., and Dunham, M.J. (2017). The dynamic three-dimensional organization of the diploid yeast genome. eLife *6*.
Kremer, S.B., and Gross, D.S. (2009). SAGA and Rpd3 chromatin modification complexes dynamically regulate heat shock gene structure and expression. J Biol Chem *284*, 32914-32931.
Larson, A.G., Elnatan, D., Keenen, M.M., Trnka, M.J., Johnston, J.B., Burlingame, A.L., Agard, D.A., Redding, S., and Narlikar, G.J. (2017). Liquid droplet formation by HP1alpha suggests a role for phase separation in heterochromatin. Nature *547*, 236-240.
Lee, K., Hsiung, C.C., Huang, P., Raj, A., and Blobel, G.A. (2015). Dynamic enhancer-gene body contacts during transcription elongation. Genes Dev *29*, 1992-1997.
Li, G., Ruan, X., Auerbach, R.K., Sandhu, K.S., Zheng, M., Wang, P., Poh, H.M., Goh, Y., Lim, J., Zhang, J.*, et al.* (2012). Extensive promoter-centered chromatin interactions provide a topological basis for transcription regulation. Cell *148*, 84-98.
Lupianez, D.G., Kraft, K., Heinrich, V., Krawitz, P., Brancati, F., Klopocki, E., Horn, D., Kayserili, H., Opitz, J.M., Laxova, R.*, et al.* (2015). Disruptions of topological chromatin domains cause pathogenic rewiring of gene-enhancer interactions. Cell *161*, 1012-1025.
Metz, A., Soret, J., Vourc'h, C., Tazi, J., and Jolly, C. (2004). A key role for stress-induced satellite III transcripts in the relocalization of splicing factors into nuclear stress granules. Journal of cell science *117*, 4551-4558.
Morimoto, R.I. (1998). Regulation of the heat shock transcriptional response: cross talk between a family of heat shock factors, molecular chaperones, and negative regulators. Genes Dev *12*, 3788-3796.
Osborne, C.S., Chakalova, L., Brown, K.E., Carter, D., Horton, A., Debrand, E., Goyenechea, B., Mitchell, J.A., Lopes, S., Reik, W.*, et al.* (2004). Active genes dynamically colocalize to shared sites of ongoing transcription. Nat Genet *36*, 1065-1071.
Papantonis, A., Kohro, T., Baboo, S., Larkin, J.D., Deng, B., Short, P., Tsutsumi, S., Taylor, S., Kanki, Y., Kobayashi, M.*, et al.* (2012). TNFalpha signals through specialized factories where responsive coding and miRNA genes are transcribed. EMBO J *31*, 4404-4414.

Papantonis, A., Larkin, J.D., Wada, Y., Ohta, Y., Ihara, S., Kodama, T., and Cook, P.R. (2010). Active RNA polymerases: mobile or immobile molecular machines? PLoS Biol *8*, e1000419.
Park, S.K., Xiang, Y., Feng, X., and Garrard, W.T. (2014). Pronounced cohabitation of active immunoglobulin genes from three different chromosomes in transcription factories during maximal antibody synthesis. Genes Dev *28*, 1159-1164.
Rao, S.S., Huntley, M.H., Durand, N.C., Stamenova, E.K., Bochkov, I.D., Robinson, J.T., Sanborn, A.L., Machol, I., Omer, A.D., Lander, E.S.*, et al.* (2014). A 3D map of the human genome at kilobase resolution reveals principles of chromatin looping. Cell *159*, 1665-1680.
Rutledge, M.T., Russo, M., Belton, J.M., Dekker, J., and Broach, J.R. (2015). The yeast genome undergoes significant topological reorganization in quiescence. Nucleic Acids Res *43*, 8299-8313.
Schoenfelder, S., Sexton, T., Chakalova, L., Cope, N.F., Horton, A., Andrews, S., Kurukuti, S., Mitchell, J.A., Umlauf, D., Dimitrova, D.S.*, et al.* (2010). Preferential associations between co-regulated genes reveal a transcriptional interactome in erythroid cells. Nat Genet *42*, 53-61.
Solis, E.J., Pandey, J.P., Zheng, X., Jin, D.X., Gupta, P.B., Airoldi, E.M., Pincus, D., and Denic, V. (2016). Defining the essential function of yeast Hsf1 reveals a compact transcriptional program for maintaining eukaryotic proteostasis. Mol Cell *63*, 60-71.
Sorger, P.K., and Pelham, H.R.B. (1988). Yeast heat shock factor is an essential DNA-binding protein that exhibits temperature-dependent phosphorylation. Cell *54*, 855-864.
Strom, A.R., Emelyanov, A.V., Mir, M., Fyodorov, D.V., Darzacq, X., and Karpen, G.H. (2017). Phase separation drives heterochromatin domain formation. Nature *547*, 241-245.
Toth-Petroczy, A., Oldfield, C.J., Simon, I., Takagi, Y., Dunker, A.K., Uversky, V.N., and Fuxreiter, M. (2008). Malleable machines in transcription regulation: the mediator complex. PLoS Comput Biol *4*, e1000243.
Weintraub, A.S., Li, C.H., Zamudio, A.V., Sigova, A.A., Hannett, N.M., Day, D.S., Abraham, B.J., Cohen, M.A., Nabet, B., Buckley, D.L.*, et al.* (2017). YY1 Is a Structural Regulator of Enhancer-Promoter Loops. Cell *171*, 1573-1588.
Wendt, K.S., and Grosveld, F.G. (2014). Transcription in the context of the 3D nucleus. Curr Opin Genet Dev *25*, 62-67.
Wong, K.H., Jin, Y., and Struhl, K. (2014). TFIIH phosphorylation of the Pol II CTD stimulates mediator dissociation from the preinitiation complex and promoter escape. Molecular cell *54*, 601-612.
Zhang, Y., Wong, C.H., Birnbaum, R.Y., Li, G., Favaro, R., Ngan, C.Y., Lim, J., Tai, E., Poh, H.M., Wong, E.*, et al.* (2013). Chromatin connectivity maps reveal dynamic promoter-enhancer long-range associations. Nature *504*, 306-310.
Zhao, J., Herrera-Diaz, J., and Gross, D.S. (2005). Domain-wide displacement of histones by activated heat shock factor occurs independently of Swi/Snf and is not correlated with RNA polymerase II density. Mol Cell Biol *25*, 8985-8999.

FIGURE LEGENDS

Figure 1. *HSP* Genes Engage in Highly Specific Intergenic Interactions

(A) Hsf1 ChIP-seq profile of a 50 kb region on Chr. XII in NHS and 5 min HS cells. Genes subjected to Taq I - 3C analysis in panel B are highlighted; physical maps are provided in Figure S1. RPKM, reads per kilobase per million mapped reads.

(B) (*Left*) Contact frequencies between the indicated regions of *UBI4, FRA1, HSP104* and *SSA2* in cells grown under NHS conditions (30°C), as determined by Taq I - 3C. Formaldehyde-crosslinked chromatin was isolated and sequentially treated with Taq I and T4 DNA ligase. Genomic DNA was purified and primers proximal to Taq I sites (Figure S1A) were used in the indicated pairwise tests. Values indicate normalized interaction frequencies, determined as previously described (Chowdhary et al., 2017) (see also Figure S2A). (*Right*) Same, except chromatin was isolated from cells exposed to a 10 min, 39°C heat shock. *HSP104* - *PAU17* contact frequencies are shown below triangulated analysis. Intensity of color is proportional to the frequency of interaction. Data are derived from two independent biological replicates (qPCR=4 for each primer combination).

(C) Physical map of Chr. XII. The rDNA repeats and *TMA10* are located on the right arm of Chr. XII, 600 kb and 300 kb from *TEL12R*, respectively. Coordinates are numbered relative to the left telomere and do not take into account the presence of rDNA.

(D) Hsf1 occupancy profile of the indicated ~20 kb region on Chr. XII. Hsf1 ChIP-seq analysis presented as in A.

(E) Intergenic interaction frequencies between *HSP104-TMA10* and *SSA2-TMA10* in NHS and 10 min HS cells. For each pairwise test, N=2, qPCR=4.

See also Figures S1 and S2.

Figure 2. Robust Interchromosomal Interactions Take Place Between Hsf1- But Not Msn2/4-Activated Genes

(A) Matrix summaries of intergenic interaction frequencies between the indicated Msn2/4-target genes in 10 min heat-shocked cells as detected by Taq I - 3C. For each pairwise test, N=2, qPCR=4.

(B) As in A, except pairwise tests were conducted between the indicated Hsf1-target genes.

(C) As in A, except intergenic interactions between Msn2/4- and Hsf1-regulated genes were determined.

(D) *(Top)* Schematic of *lacO*-tagged loci present in the heterozygous diploids in which the relative chromosomal locations of *HSP104*, *HSP12* and *PGM2* are indicated (filled circles, centromere). (*Bottom*) Percentage of *HSP104-HSP12* (solid bars) or *HSP104-PGM2* (shaded bars) cells exhibiting coalescence as determined by fixed-cell fluorescence microscopy. For *HSP104-HSP12*, 50-70 cells were evaluated per sample at each time point (N=2); for *HSP104-PMA2*, 80-100 cells were evaluated per time point (N=1). Data for *HSP104-HSP12* coalescence are from (Chowdhary et al., 2017).

(E) Distribution of distances between *HSP104* and *HSP12* (*Top*) or *HSP104* and *PGM2* (*Bottom*) in cells subjected to the indicated conditions. Depicted is the percentage of cells within the indicated distance (binned at intervals of 0.4μm) in a given population of fixed cells. *P* value was calculated by Wilcoxon rank sum test.

(F) Fluorescence microscopy of live cells harboring Hsf1-GFP (*Top*) or Msn2-GFP (*Bottom*) prior to or following application of heat for the times and temperatures indicated. Cells boxed in red are enlarged at bottom right of the respective images. Scale bar = 2 μm.

See also Figures S1 and S3.

Figure 3. DNA-Bound Hsf1 Is Both Necessary and Sufficient to Trigger Coalescence of a Pol II Gene

(A) Spot dilution analysis of BY4742-HSF1-FRB (hereafter "Hsf1-AA") cells. Five-fold serial dilutions of cells were spotted onto YPDA +/- rapamycin as indicated. Plates were incubated at 30° or 37°C for 2-3 days. WT, BY4742.

(B) Hsf1 ChIP analysis of representative *HSP* genes. Hsf1-AA cells were pretreated with rapamycin for 90 min or not as indicated, then subjected to a 10 min HS and processed for ChIP. Amplicon coordinates are provided in Table S4. Depicted are means + SD (N=2; qPCR=4).

(C and D) Taq I - 3C analysis of *HSP* intragenic and intergenic interactions in Hsf1-AA cells pretreated with rapamycin followed by 10 min heat shock. Depicted are means +SD (N=2; qPCR=4).

(E) Physical map of UAS_{HS}-*BUD3*, a chromosomal transgene harboring HSEs1-3 of *HSP82* (Erkine et al., 1999) at the position indicated.

(F) Hsf1 occupancy of *BUD3* and UAS_{HS}-*BUD3* under NHS and 10 min HS states.

(G) Summary of intragenic interactions detected within UAS_{HS}-*BUD3* in NHS and 10 min HS states (N=2; qPCR=4).

(H) Intergenic contact frequencies between the indicated genes in 10 min HS cells (N=2; qPCR=4).

See also Figures S1, S4 and S5.

Figure 4. Pol II Transcription Is Necessary But Not Sufficient to Drive Gene Coalescence

(A) *(Left)* Physical map of *HSP12* depicting the HSE and STREs within its upstream region (derived from www.yeastract.com). Coordinates are numbered with respect to *HSP12* ATG codon. *(Right)* Hsf1 ChIP-seq profile of the indicated region on Chr. VI in NHS and 5 min HS cells.

(B) Taq I - 3C analysis of intragenic interactions within *HSP12* in Hsf1-AA cells as in Figure 3C.

(C) Same as B except intergenic interactions between *HSP12* and representative Hsf1-target genes are shown.

(D) Rpb1 ChIP analysis of representative *HSP* genes in Rpb1-AA cells pretreated with rapamycin or not (as indicated) followed by a 10 min HS. Depicted are means +SD (N=2; qPCR=4).

(E and F) Taq I - 3C analysis of *HSP* intragenic and intergenic interactions in Rpb1-AA cells pretreated with rapamycin or not (as indicated) followed by a 10 min HS. Depicted are means +SD (N=2; qPCR=4).

See also Figures S1 and S6.

Figure

Chowdhary Fig. 1

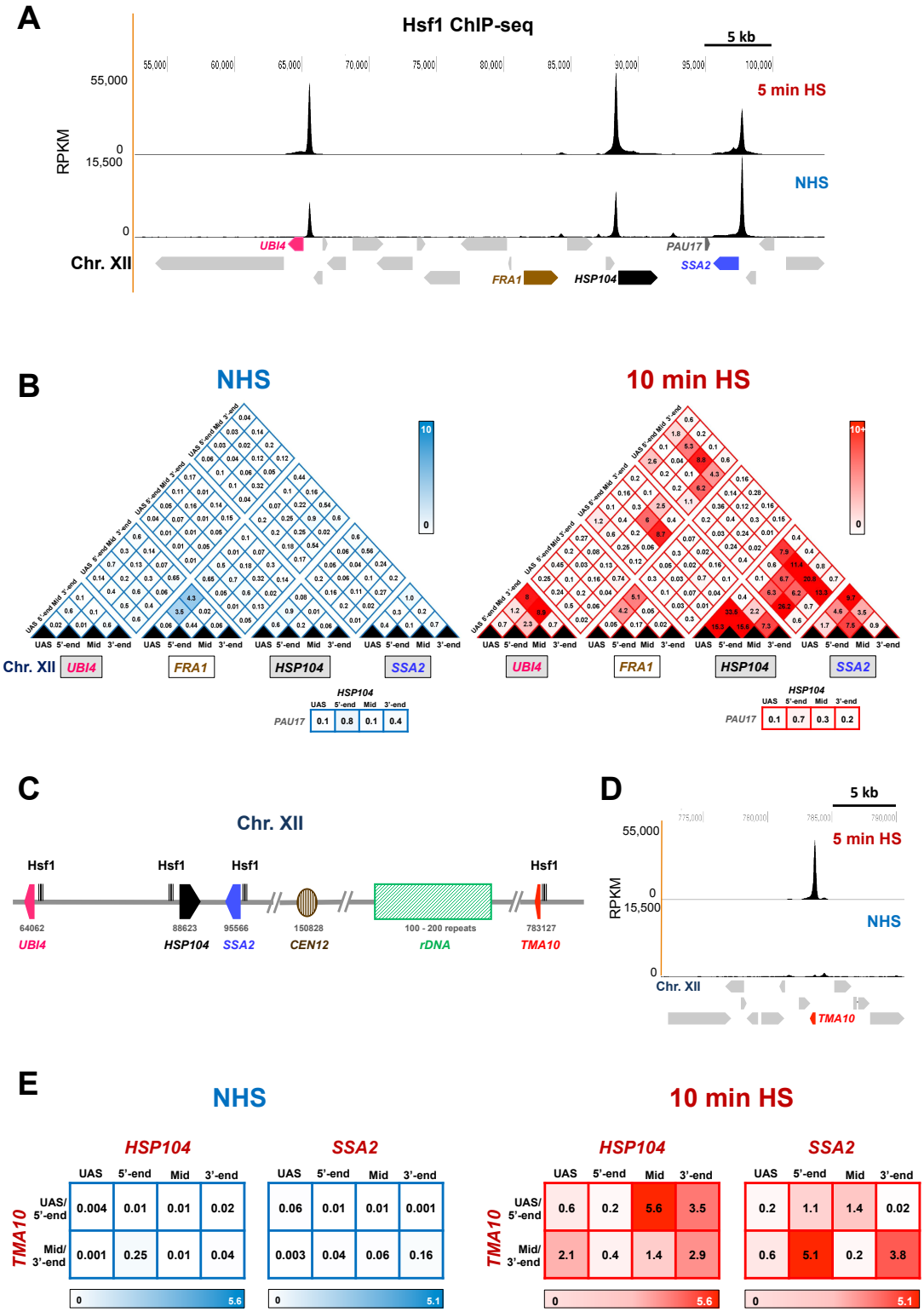

Chowdhary Fig. 2

A

CTT1 (Chr. VII)

PGM2 (Chr. XIII)	UAS	5'-end	Mid	3'-end
UAS	0.18	1	0.16	0.09
5'-end	0.03	0.15	0.14	0.2
Mid	0.35	0.14	1.2	0.03
3'-end	0.07	0.5	0.07	0.6

0 — 5

RTN2 (Chr. IV)

PGM2 (Chr. XIII)	UAS /5'-end	Mid	3'-end
UAS	0.02	0.08	0.01
5'-end	0.2	0.2	0.13
Mid	0.1	0.03	0.03
3'-end	0.2	0.17	0.23

0 — 5

RTN2 (Chr. IV)

CTT1 (Chr. VII)	UAS /5'-end	Mid	3'-end
UAS	0.01	0.04	0.01
5'-end	0.1	0.33	0.2
Mid	0.05	0.06	0.06
3'-end	0.14	0.49	0.05

0 — 5

B

HSP104 (Chr. XII)

SSA4 (Chr. V)	UAS	5'-end	Mid	3'-end
UAS	0.7	3.5	1	4.8
5'end	0.3	0.08	7.1	0.02
Mid	1.8	0.5	0.7	0.6
3'-end	0.4	4.5	3.3	1

0 — 7.1

HSP104 (Chr. XII)

HSP12 (Chr. VI)	UAS	5'-end	Mid	3'-end
UAS	0.3	1.1	8.4	4
5'end/ Mid	0.33	0.9	0.03	0.13
3'-end	0.24	0.4	0.02	0.1

0 — 8.4

HSP82 (Chr. XVI)

SSA2 (Chr. XII)	UAS	5'-end	Mid	3'-end
UAS	0.01	0.03	0.1	1.4
5'end	0.06	0.07	2.4	9.5
Mid	0.22	0.15	0.3	0.9
3'-end	0.1	1.1	0.2	0.9

0 — 9.5

C

PGM2

HSP104	UAS	5'-end	Mid	3'-end
UAS	0.18	0.07	0.8	1.1
5'-end	0.3	0.07	0.4	0.17
Mid	0.12	0.09	0.02	0.08
3'-end	0.2	0.02	0.2	0.6

0 — 5

CTT1

HSP82	UAS	5'-end	Mid	3'-end
UAS	0.03	0.01	0.64	0.02
5'-end	0.13	0.97	0.03	0.18
Mid	0.01	0.01	0.01	0.2
3'-end	0.74	0.04	0.13	0.27

0 — 5

RTN2

HSP104	UAS /5'-end	Mid	3'-end
UAS	0.02	0.05	0.35
5'-end	0.12	0.48	0.22
Mid	0.02	0.26	0.2
3'-end	0.28	0.35	0.17

0 — 5

D

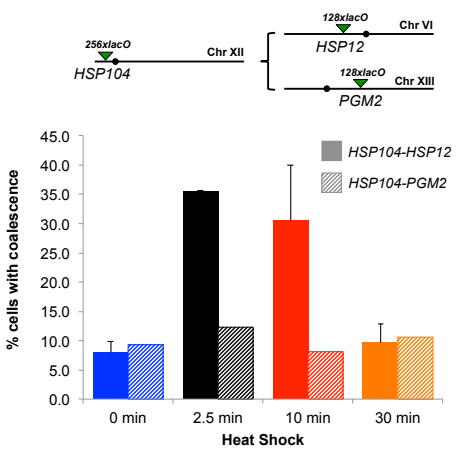

E

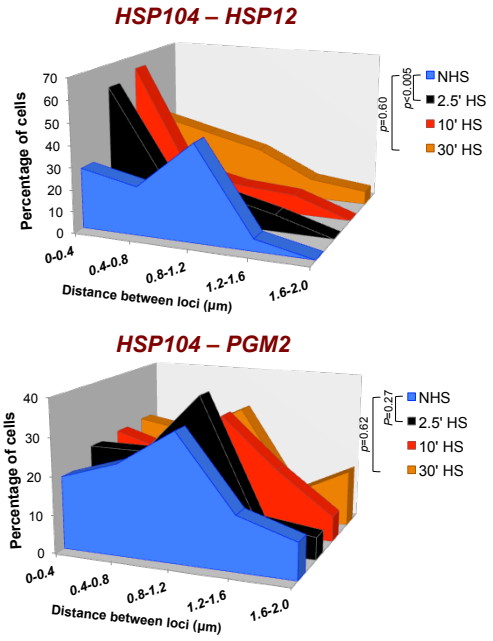

F

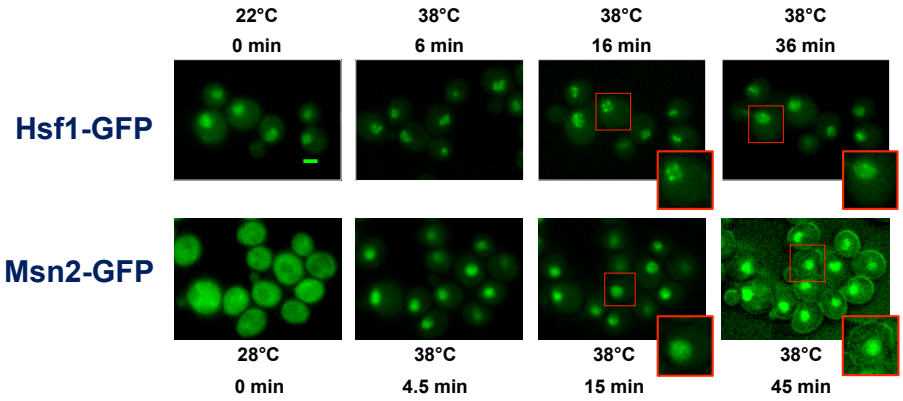

Chowdhary Fig. 3

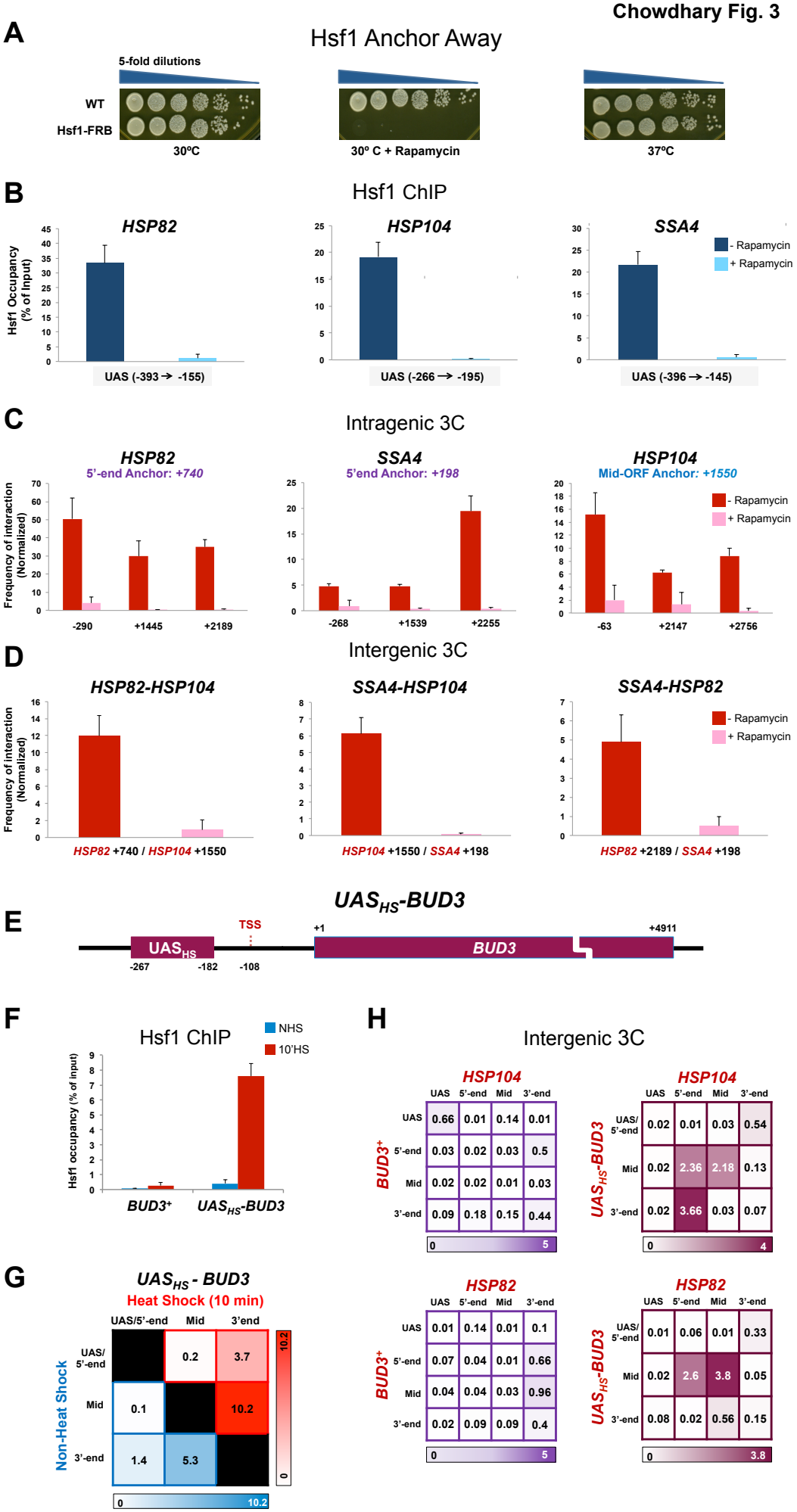
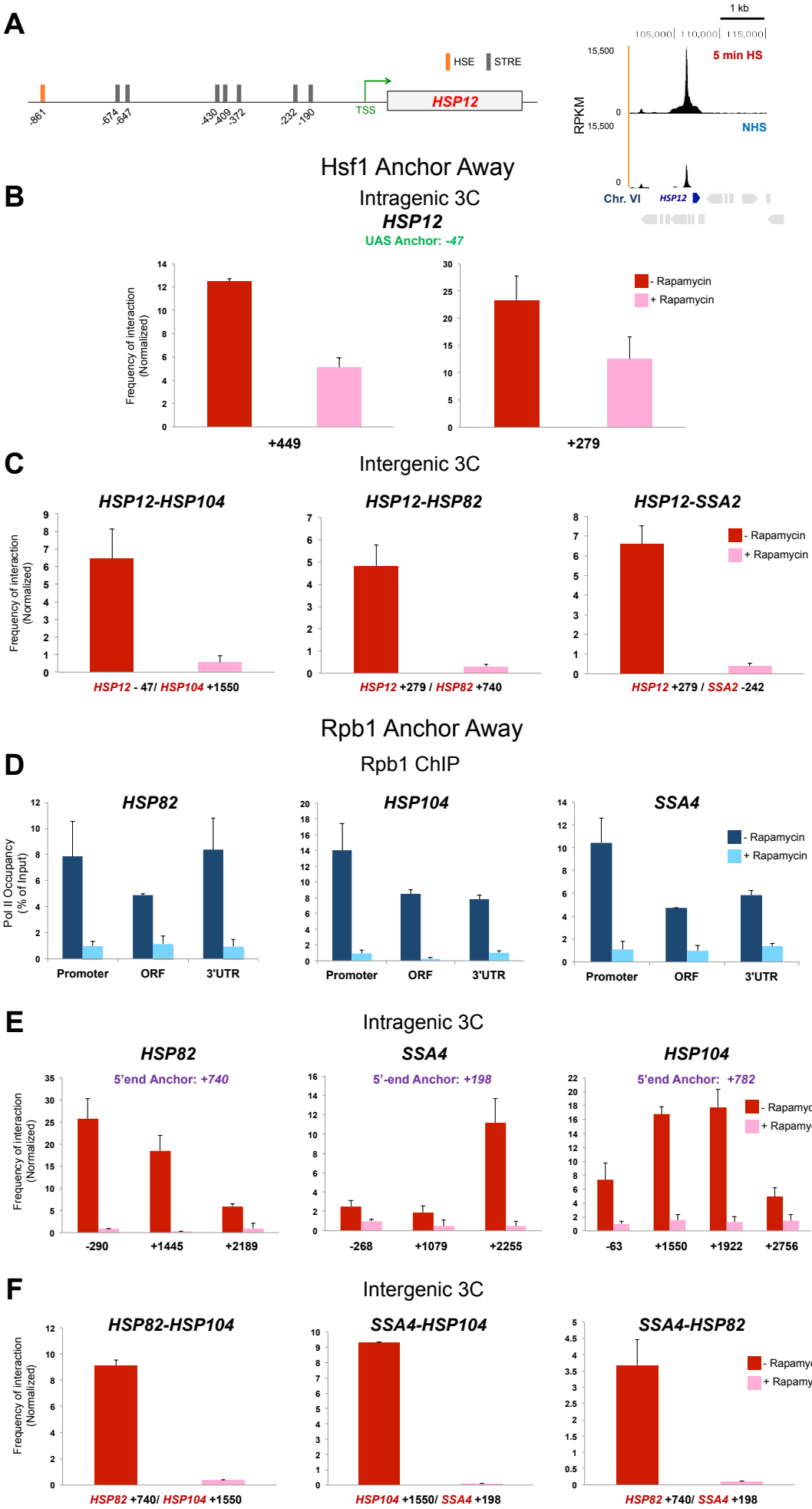
Chowdhary Fig. 4